Nonstationary Time-Series Analysis: Accurate Reconstruction of Driving Forces

P. F. Verdes, P. M. Granitto, H. D. Navone, and H. A. Ceccatto

Instituto de Física Rosario, Consejo Nacional de Investigaciones Científicas y Técnicas and Universidad Nacional de Rosario, Boulevard 27 de Febrero 210 Bis, 2000 Rosario, República Argentina

(Received 5 May 2001; published 4 September 2001)

We propose a simple method for the accurate reconstruction of slowly changing external forces acting on nonlinear dynamical systems. The method traces the evolution of the external force by locally linearizing the map dependency with the shifting parameter. Application of our algorithm to synthetic data corresponding to discrete models of evolving ecosystems shows an accuracy that outperforms those of previous methods in the literature. In addition, an application to the real-world sunspot time series recovers recently reported changes in solar activity during the last century.

DOI: 10.1103/PhysRevLett.87.124101 PACS numbers: 05.45.Tp, 95.75.Wx

Most real-world time series have some degree of nonstationarity due to external perturbations of the observed system. Furthermore, natural dynamics are often complex enough to comprise multiple time scales, so that for short observational periods the effective degrees of freedom with the largest scales act as external perturbations for the fastest observed modes. In spite of this, the vast literature on nonlinear time-series analysis and the techniques developed from the theory of dynamical systems [1] mostly rely on the stringent condition of stationarity. In recent years, however, an increasing effort has been devoted to devise methods for nonstationary time series analysis [2,3]. Recent works have addressed the question of the proper characterization of nonstationarity [4], caused either by slow continuous perturbations (driving forces) or by abrupt discrete changes in the dynamics [2,5]. Furthermore, delay embedding ideas have been extended and used to cope with nonstationarity [6]. In addition, there have been applications that range from monitoring physiological and mechanical signals [7] to extracting messages from a chaotic background [8]. Nonstationary time series analysis is also of major relevance for ecosystem modeling [9] and population dynamics under changing environmental conditions [10].

In this Letter we focus on the accurate reconstruction of external driving forces. This problem has already been discussed by Casdagli [2] using recurrence plots but, as this author himself states, this method is not very accurate. A more efficient method based on the calculation of cross-prediction errors has been proposed by Schreiber [3]. Here we present a simpler method to trace parameter variations from the nonstationary dynamics of complex systems, and assess its performance by applying it to synthetic data from ecosystem models. Furthermore, we discuss a concrete application to the real-world sunspot time series, obtaining results that agree with observed changes in solar dynamics during the last century [11].

Consider an observational record with N data values corresponding to a process generated by a deterministic dynamical system. We want to model this process in a d-dimensional pseudophase space according to $x_{t+1} = f(\mathbf{x}_t, \alpha_t)$, where $\mathbf{x}_t = (x_t, x_{t-1}, \ldots, x_{t-d+1})$ and time t is measured in units of the lag τ between observations. Here α_t accounts for the effects of either an external driving force or other internal degrees of freedom varying on large time scales T not modeled by f. Then, if we split the data into N_{int} (possibly overlapping) intervals of M points each, for $M\tau \ll T$ we can write $x_{t+1}^{(m)} \simeq f(\mathbf{x}_t^{(m)}, \alpha^{(m)})$, where $\alpha^{(m)}$ is the mean value of the parameter in the mth interval considered and now t runs only on points of this interval. For a smooth dependence of f with α we can approximate $x_{t+1}^{(m)} - f(\mathbf{x}_t^{(m)}, \alpha^{(k)}) \simeq \frac{\partial f}{\partial \alpha}(\mathbf{x}_t^{(m)}, \alpha^{(k)})\,(\alpha^{(m)} - \alpha^{(k)})$, which should be valid for intervals k and m close enough (in practice they can be taken with a substantial overlap to fulfill this condition). Averaging over all t in interval m we obtain

$$E_k^m = A_k^m \Delta\alpha_k^m , \tag{1}$$

where we have introduced the notation $E_k^m = \langle x_{t+1}^{(m)} - f(\mathbf{x}_t^{(m)}, \alpha^{(k)})\rangle_t$, $A_k^m = \langle \frac{\partial f}{\partial \alpha}(\mathbf{x}_t^{(m)}, \alpha^{(k)})\rangle_t$, and $\Delta\alpha_k^m = \alpha^{(m)} - \alpha^{(k)}$. Here the subindex k is fixed and denotes the interval used as reference, while the running superindex m describes the actual temporal variation of the driving force. Assume now that the M data points in interval k cover the attractor well enough to allow modeling $f(\bullet, \alpha^{(k)})$, obtaining a predictor $\hat{f}(\bullet, \alpha^{(k)})$ and estimates $\hat{E}_k^m$. Even in this case the system of Eq. (1) cannot be solved for the $\Delta\alpha$'s because we do not have an estimate for A_k^m. However, since to the same order of approximation we can replace $\frac{\partial f}{\partial \alpha}(\mathbf{x}_t^{(m)}, \alpha^{(k)})$ by $\frac{\partial f}{\partial \alpha}(\mathbf{x}_t^{(m)}, \alpha^{(m)})$, we can drop the subindex k in A_k^m. Thus, the system (1) can be solved up to a scale transformation. In particular, for contiguous intervals ($m = k + 1$) and taking A^1 as the parameter of the unknown scale transformation, the solution is

$$\Delta\alpha_k^{k+1} = (-1)^{k+1} \frac{\hat{E}_{k+1}^k}{A^1} \prod_{r=1}^{k-1} \left(\frac{\hat{E}_{r+1}^r}{\hat{E}_r^{r+1}} \right). \tag{2}$$

Notice that the ratio $E_{r+1}^r / E_r^{r+1} = -1 + O(\Delta\alpha_r^{r+1})$.

According to the above discussion, we propose the following procedure for reconstructing α: Choose a

segment k and use its iterates to construct a model $\hat{f}(\bullet, \alpha^{(k)})$. Then, compute the average prediction errors $\hat{E}_k^m$ for $m = k \pm 1$. Repeat for all possible k and reconstruct the driving force up to arbitrary scale A^1 and shift $\alpha^{(1)}$ according to Eq. (2). Following this procedure, even for a perfect modeling technique there are methodological errors due to (i) the replacement on each interval of the varying parameter α by its mean value, and (ii) the local linear approximation used to obtain Eq. (1). To test these questions we have considered three well-known, single-species discrete chaotic ecosystem models, whose dynamics under external forcing has been discussed in Ref. [9]. These models are given by $x_{t+1} = \mu x_t(1 - x_t)$, $x_{t+1} = x_t \exp[r(1 - x_t/K)]$, and $x_{t+1} = \lambda x_t/(1 + x_t)^{\beta}$, corresponding, respectively, to the logistic, Moran-Ricker, and Hassell maps. The logistic equation is well known beyond mathematical biology, while the Moran-Ricker and Hassell maps have been used in the analysis of insect and fish records. We drove the parameters μ and λ to exemplify the case of a linear dependency of the maps with the external force, and the parameters K and β to study the nonlinear problem. In all these cases we have considered a variation given by $\alpha_t = C_\alpha \cos(2\pi t/T)\exp(-2\pi t/T) + B_\alpha$, and used nonoverlapping intervals, i.e., $N = MN_{\text{int}}$. The constant C_α gives the force strength, and for each map it was taken as large as possible without collapsing the attractor to a trivial structure nor producing divergent behavior [12]. The task is, of course, to reconstruct α_t up to this amplitude and the constant displacement B_α. We took $T = N/2$, so that the profile of the force is the same independently of the record length considered, and varied the number of intervals $N_{\text{int}} = 10{-}40$ to split this profile. For simplicity, the number of iterates within each interval was fixed to $M = 1000$ for all maps, which allows modeling their respective chaotic dynamics. Notice that according to this experimental setting N_{int} is controlling the validity of the approximations made above (essentially the fact that the driving force has a small change between neighboring intervals). We used radial basis function (RBF) networks [1] to model the maps, and all the results below correspond to an average over 20 independent realizations of the whole process [13].

In order to appraise the performance of the reconstruction method based on Eq. (2), we computed the normalized mean squared error (NMSE) between the original and reconstructed forces, i.e., the MSE divided by the force variance. First, in order to explore the error due to the assumption of a switching dynamics between intervals instead of the real continuous parameter change, in Fig. 1 we plot the NMSE as a function of N_{int} for the logistic map (for which the linear approximation in α, the other source of error, is exact). In this figure we include also the corresponding results from Schreiber's method [3,14] using the same RBF models. Our approach shows an average error more than 2 orders of magnitude smaller and, as expected, it tends to decrease with N_{int} (it drops almost 1 order of magnitude in going from 10 to 40 intervals). A more thorough comparison between both methods is given in Table I, where we present results in the least favorable situation for our approach ($N_{\text{int}} = 10$) for the three ecosystem maps considered. Column (a) corresponds to the ideal case of switching dynamics and perfect modeling, where the true dynamics are used to compute E_k^m and we replace the driving force on each interval by its mean value. These figures are a better comparison between the relative accuracy of both reconstruction algorithms at a methodological level (in this case, for maps with linear dependency on the shifting parameter the error in our approach is exactly zero). Furthermore, column (b) gives the corresponding results in the real situation of continuous parameter drift and RBF modeling. Both for the ideal case and for the real problem with linear dependency our algorithm produces NMSE values much smaller (1 order of magnitude or even less) than Schreiber's method. For nonlinear dependencies our results have also smaller errors and, as discussed below, they can be further reduced by taking advantage of the possibility of using overlapping intervals.

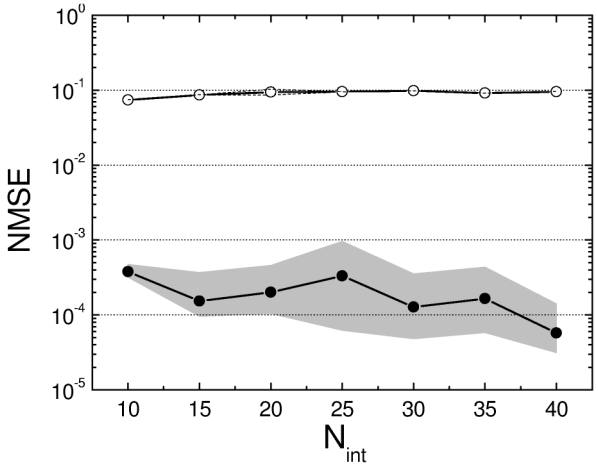

FIG. 1. NMSE as a function of the number of intervals N_{int} for the logistic map. Open dots correspond to the method of Ref. [3]; full dots are the results from Eq. (2). Gray area represents estimated errors.

We have considered the Hassel and Moran-Ricker equations and performed the same study as above with N_{int} varying from 10 to 191, keeping always the original $N = 10\,000$ data points. This corresponds to contiguous intervals having a fraction of common points varying from 0% to 95%. The method in Ref. [3] slightly improves

TABLE I. Average NMSE and their standard deviations. (a) Switching dynamics and perfect modeling; (b) Continuous parameter drift and RBF modeling.

	(a) NMSE (10^{-2})		(b) NMSE (10^{-2})	
Map	Ref. [3]	This work	Ref. [3]	This work
Log	9.2 ± 0.1	0	7.4 ± 0.1	0.04 ± 0.02
H(λ)	8.5 ± 0.2	0	5.1 ± 0.4	0.08 ± 0.03
H(β)	9.7 ± 0.4	1.6 ± 0.1	4.0 ± 0.5	1.8 ± 0.5
M-R	8.3 ± 0.5	0.2 ± 0.2	6.0 ± 0.4	1.4 ± 1.0

with increasing overlaps (see Fig. 2), but the results obtained using Eq. (2) deteriorate because the $\hat{E}_k^m$ are smaller and tend to have large relative errors. The solution (2) is unstable to these modeling errors, something which becomes particularly acute near stationary points of the driving force where $\hat{E}_k^m \sim 0$. A way to cope with these problems is to write several systems of equations like (1), $E_k^m = A^m \Delta\alpha_k^m$, with $|m-k| = 1, 2, \ldots, n$, considering error estimates $\hat{E}_k^m$ between neighboring but noncontiguous intervals. Now, since $\Delta\alpha_k^m = \sum_{r=k}^{m-1} \Delta\alpha_r^{r+1}$, all the solutions with $|m-k| > 1$ provide constraints for the one-step shifts $\Delta\alpha_k^{k+1}$. We have then $2(N_{\text{int}} - 1)$ unknown quantities $\Delta\alpha_k^{k+1}$ and $A^{k+1}(k = 1, N_{\text{int}} - 1)$, and $2n(N_{\text{int}} - \frac{n+1}{2})$ equations to be fulfilled. This allows us to obtain a more stable solution by solving the system in a mean-square-error sense, which should compensate for uncorrelated modeling errors in $\hat{E}_k^m$. We have implemented a simple gradient-descent minimization of the error function

$$\varepsilon = \sum_{r=1}^{n} \Bigg[\sum_{k=1}^{N_{\text{int}}-r} P_r (\hat{E}_k^{k+r} - A^{k+r} \Delta\alpha_k^{k+r})^2 + \sum_{k=r+1}^{N_{\text{int}}} P_r (\hat{E}_k^{k-r} + A^{k-r} \Delta\alpha_{k-r}^{k})^2 \Bigg] + \eta \sum_{k=1}^{N_{\text{int}}-1} \Delta^2 A^k, \tag{3}$$

where $\Delta A^k = A^{k+1} - A^k$. The η term forces the method to seek for smooth solutions, as is usually done for ill-defined problems. Here P_r is a normalized arbitrary weight that can be used to reduce the importance of equations involving intervals farther apart. The simplest case, and the one we have explored in detail in this work, corresponds to square systems ($P_r = \delta_{r,1}$), where the minimization of ε produces more regular results than the exact solution (2). Notice that this way of solving the problem can deal with stationary regions in the driving force. Furthermore, the effects of accidentally large modeling errors in $\hat{E}_k^m$ will be moderated by the η term. Figure 2 shows that the NMSE obtained in this way for both the Hassel and Moran-Ricker maps have roughly an exponential decay with the intervals' overlap. For large overlaps, the minimization of ε for square systems produces again NMSE 1 order of magnitude smaller than Schreiber's method. We have checked that different initializations of A^k and $\Delta\alpha_k^{k+1}$ do not sensibly change these results [15]. A brief comment concerning η: As expected, for small values of this parameter the solutions obtained from different initializations have erratic NMSE, while for very large η the A^k's remain pinned to 1; in between, there is a large plateau in NMSE as a function of η for $\eta \sim 1$ that we have taken as an indication of a stable solution.

We have observed that the consideration of overdetermined systems leads to a further small error reduction when $n = 2$ or 3. Beyond that, the use of farther apart intervals spoils the local nature of our algorithm. However, having overdetermined systems opens up the more interesting possibility of solving the problem for the simultaneous external drive of *two* or more parameters. This situation is by no means unusual for real systems and, to our knowledge, it has not been explored in depth in the literature. Space limitations prevent us from discussing here a simple extension of the algorithm above described to treat this problem.

Finally, we present an application to the real-world sunspot time series, which has been suggested to correspond to a driven nonlinear oscillator [16]. To provide a more stringent test for the algorithm we have removed from this series trivial features related to weak (linear) nonstationarities. For this, we have segmented the solar cycles and normalized their amplitudes to 1, so that after reuniting these pieces the resulting time series has no amplitude modulation nor average drift (see Fig. 3, upper panel). The application of the reconstruction algorithm leads to the noisy result (thin line) shown in the lower panel of Fig. 3; the same algorithm applied to the original time series gives the result indicated by the thick line. Both results have been smoothed with a moving window of $M = 33$ points ($\sim$3 solar cycles), corresponding to the length of the intervals used. The small differences are due to the arbitrary breaking into pieces and normalizing process performed on the series, but the overall result is quite the same. In this case we have modeled the dynamics using ensembles of feedforward neural networks [17], and considered $N_{\text{int}} = 297$ intervals (97% of overlap),

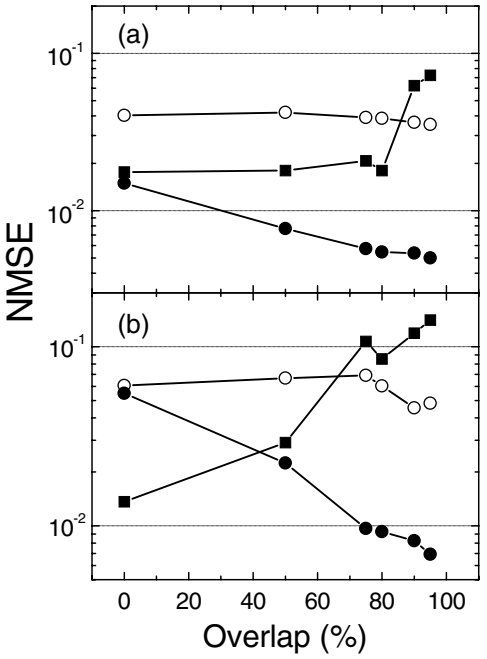

FIG. 2. NMSE as a function of the degree of overlap between contiguous intervals. (a) Hassel map; (b) Moran-Ricker map. Full squares and dots correspond, respectively, to the results obtained from Eq. (2) and by minimization of Eq. (3); open dots are results of the method in Ref. [3].

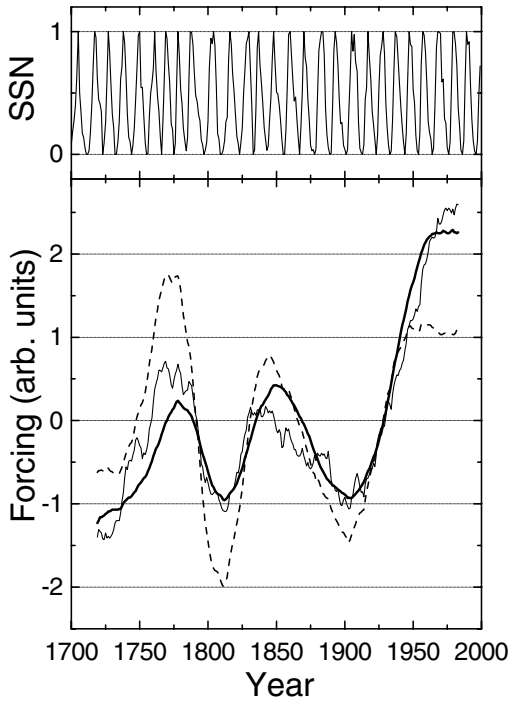

FIG. 3. Driving force for the sunspot dynamics. Upper panel: normalized sunspot series. Lower panel: reconstructed force from the original sunspot record (thick full line) and from the normalized series (thin full line), obtained by minimization of Eq. (3). The dashed line gives the result for the normalized series using the method in Ref. [3].

embedding dimension $d = 3$ and time lag $\tau = 1$. Notice that there is a perturbation with a period of $\sim$100 years that corresponds to the previously empirically determined Gleissberg cycle [18] and, more interestingly, also a rise in the perturbation amplitude in the last century. The ratio between the two more recent maxima gives $\sim$2.34, in surprising coincidence with the factor 2.31 for the increase in the sun's coronal magnetic field since 1901, recently estimated from measurements of the near-Earth interplanetary magnetic field [11]. This effect has been attributed to chaotic changes in the dynamo that generates the solar field. Implications of our findings on this problem deserve a further investigation. For comparison, in the lower panel of Fig. 3 we give also the result obtained using the method in Ref. [3] (dashed line), which fails to account for this change in amplitude.

In conclusion, we have proposed a simple and very transparent method for the accurate reconstruction of driving forces in nonstationary time series. We have shown, using synthetic data from forced chaotic ecosystems maps, that our method outperforms similar algorithms existing in the literature. Moreover, a concrete application to the analysis of the sunspot time series reveals changes in the solar dynamics which are in agreement with other recent estimations. Details of all the above calculations will be published elsewhere. The algorithm here proposed can be extended to trace the simultaneous variation of several parameters, something that to our knowledge has been only partially explored in the literature. Work in this direction is in progress.

[1] H. Kantz and T. Schreiber, *Nonlinear Time Series Analysis,* Cambridge Nonlinear Science Series 7 (Cambridge University Press, Cambridge, 1997).
[2] M. Casdagli, Physica (Amsterdam) **108D**, 12 (1997).
[3] T. Schreiber, Phys. Rep. **308**, 1 (1999).
[4] R. Manuca and R. Savit, Physica (Amsterdam) **99D**, 134 (1996); T. Schreiber, Phys. Rev. Lett. **78**, 843 (1997).
[5] F. Lombard and J. D. Hart, in *Change-Point Problems,* edited by E. Carlstein, H.-G. Muller, and D. Siegmund, IMS Lecture Notes-Monograph Series, Vol. 23 (Institute of Mathematical Statistics, Hayward, CA, 1994); M. B. Kennel, Phys. Rev. E **56**, 316 (1997).
[6] J. Stark, J. Nonlinear Sci. **9**, 255 (1999); R. Hegger *et al.,* Phys. Rev. Lett. **84**, 4092 (2000).
[7] J. Stark and B. V. Arumugan, Int. J. Bifurcation Chaos Appl. Sci. Eng. **2**, 413 (1992); L. M. Hively, P. C. Gailey, and V. A. Protopopescu, Phys. Lett. A **258**, 103 (1999).
[8] K. M. Short, Int. J. Bifurcation Chaos Appl. Sci. Eng. **7**, 1579 (1997).
[9] D. Summers, J. G. Cranford, and B. P. Healey, Chaos Solitons Fractals **11**, 2331 (2000).
[10] D. J. D. Earn *et al.,* Science **287**, 667 (2000).
[11] M. Lockwood, R. Stamper, and M. N. Wild, Nature (London) **399**, 437 (1999).
[12] In particular, we took $B_\mu = 3.8$, $C_\mu = 0.045$, $B_K = 1$, $C_K = 0.9$, $B_\lambda = 100$, $C_\lambda = 30$, and $B_\beta = 10$, $C_\beta = 2$. For the Moran-Ricker map we set $r = 3.7$.
[13] We have not performed a particularly careful modeling of the dynamics; for instance, we used 1 input and 6 hidden nodes for all the maps. Consequently, the results obtained might be further improved by using better modeling strategies.
[14] R. Hegger, H. Kantz, and T. Schreiber, Chaos **9**, 413 (1999).
[15] We have minimized ε starting from equally distributed values between 0 and 2 for A^k and between -0.1 and 0.1 for $\Delta\alpha_k^{k+1}$. The quoted results correspond to an average over 20 different runs of the whole algorithm.
[16] M. Palus and D. Novotna, Phys. Rev. Lett. **83**, 3406 (1999).
[17] *Combining Artificial Neural Nets: Ensemble and Modular Multi-Net Systems,* edited by A. J. C. Sharkley, Perspectives in Neural Computing (Springer-Verlag, London, 1999).
[18] W. Gleissberg, Solar Phys. **2**, 231 (1967); A. García and Z. Mouradian, *ibid.* **180**, 495 (1998).